PHOTO CATALYTIC DEGRADATION OF Ag-TiO_2 NANOTUBES BY REDUCTION METHODS

M.DEEPA[1],SANGEETHA.VS[2],P.LAVANYA[3],M.MAHALAKSHMI[4]

ABSTRACT

the photocatalytic activity of, Ag NPs loaded TiO_2 nanorods and spheres prepared through simple hydrothermal and solvothermal methods towards photocatalytic degradation of methylene blue. It is planned to synthesis TiO_2 NRs and TiO_2 NSs via hydrothermal and solvothermal method followed by deposition of Ag through chemical reduction method. The structure and morphology of Ag-TiO_2 are characterized through X-ray diffraction analysis (XRD), diffuse reflectance spectra (DRS) and Transmission electron microscopy (TEM). The photocatalytic activity of TiO_2-Ag nanorods and nanospheres is also compared

.Photocatalysis is a promising technology in the field of green technology. Photocatalysis is a catalytic process occurring at the surface of semiconductor materials under the irradiation of photons. It is an important chemical process that underpins the development of critical renewable energy and environmental technology such as photocatalytic water/air purification, hydrogen production from water splitting, and high efficiency/low cost solar cells. Currently the practical applications of this very attractive photocatalytic technique are, however, greatly restricted due to low separation probability of the photo-induced electron-hole pairs in the most stable semiconductor photocatalysts. Therefore, the big challenge for the researchers in the field of photocatalysis is to develop the photocatalysts that enhance the charge carriers separation providing industrial application for environment remediation and hydrogen production.

Photocatalytic Oxidation

Efficient physiochemical remediation methods that mineralize recalcitrant organic pollutants through in situ generation of reactive radicals have been intensively studied and reviewed [1-3]. Many of them are photochemical process that is based on photo-induced electron transfer processes, among which photocatalysis is the most extensive method. The photocatalysis can be defined as "A chemical reaction induced by photo-absorption of solid material or "photocatalyst," which remains unchanged during the reaction". work has been made possible ever since the discovery of water electrolysis by means of the titanium dioxide [4].

. TiO_2 and ZnO as photocatalyst

The scientific and engineering interest in the application of semiconductor photocatalysis has grown dramatically over the last decades [5-9]. Several simple oxide and sulfide semiconductor have bandgap energies sufficient for promoting or catalyzing a wide range of chemical reactions of environmental interest. The primary criterion for good semiconductor

photocatalysts for organic pollutant degradation is that the redox potential of the $H_2O/^{\cdot}OH$ ($^{\cdot}OH= {}^{\cdot}OH+e^-$; E^0=-2.8 ev) couple lies within the bandgap domain of the material and that the material is stable over prolonged periods of time. Among the different semiconductors such as TiO_2 (Eg=3.2ev), WO_3 (Eg=2.8ev), $SrTiO_3$ (Eg=3.2ev), α-Fe_2O_3 (Eg=3.1ev), ZnO (Eg=3.2ev), and ZnS (Eg=3.6ev), investigated for photocatalysis applications, TiO_2 and ZnO (ZnO is a well-known alternative for TiO_2) have been proven to be the most suitable photocatalyst for the removable of wide range of organic contaminants. TiO_2 is inexpensive, biologically and chemically inert, have large bandgap, have high photosensitivity and are stable with respect to photo-corrosion and chemical photocatalyst has been applied to a variety of problems of environmental interest such as water and air purification,[10-13]destruction microorganism, [14] photo-splitting of water for the production of hydrogen [15] and oil spills cleanup [16].

Photocataytic oxidation at the liquid – solid interface on TiO_2 and ZnO catalysts

TiO_2 and ZnO are used as a photocatalyst for the efficient oxidation of organics during treatment of polluted waters. For instance, environmentally highly toxic chlorobenzene undergoes mineralization over TiO_2 [17,18]. Continuous bandgap irradiation of aqueous semiconductor dispersion excites an electron from valence band to the conduction band thereby creating an electron-hole pair. The electrons possess the reducing power of the conduction band energy and the holes have the oxidizing power of the valence band energy. From the band –edge position of the valence band and conduction band, the redox capability of a photo-excited semiconductor particle in the aqueous solution can be estimated. The bulk photoelectrons and photo-holes can recombine to produce thermal energy, or rapidly migrate to the surface and react with adsorbed species at the surface. In a steady state photocatalytic reaction, the rate of oxidation by the holes has to be balanced by the rate of reduction by the electrons. Either of these reactions can be rate determining. Although, the above physical events are generally accepted as the initial step for the photocatalytic oxidation process, the subsequent chemical events at the liquid-solid interface remain an ambiguous and controversial issue. The trapped holes have been proposed to directly oxidize adsorbate molecule or to react with surface hydroxyl groups to produce hydroxyl radicals which are strong oxidizing agent [19]. The trapped electrons are believed to react with re-adsorbed molecular oxygen to produce O_2^- and $O_2^{\cdot}$ anions. They may directly oxidize organic species, protonate to generate hydro-peroxide radicals and hydroxyl radicals or further react with more trapped electron eventually to form water. The oxygen plays a specific role during photocatalytic oxidation in addition to scavenging the trapped electron.

One dimensional nanostructure TiO_2 and ZnO

Nanoscience involves the study of materials having at least one of the dimensions in the range 1-100nm. Now a days modern chemist is exploring ways to

obtain such controlled material at the nanometer scale. Interest in nanomaterial is due to the fact that they exhibit some novel properties which cannot be observed in their bulk counterparts. Also, the properties of nanomaterials can be tuned by simply controlling the particle size and shape. It has been revealed both theoretically and experimentally that the electronic band of a crystal is gradually quantized as the crystal-size is reduced, resulting in an increase in the bandgap energy. Moreover, electron transport processes are significantly influenced by the size of the nanocrystals. Similarly, in the determination of their properties the shape of nanocrystals plays a crucial parameter. The shape of nanocrystals may be simply classified by their dimensionality [20]. Fig.3 illustrates the basic geometrical motifs of nanocrystals: Zero-dimensional (0D) isotropic spheres, cubes, and polyhedrons; one-dimensional (1D) tubes, fibers, rods and wires; two-dimensional (2D) discs, prisms, and plates; three-dimensional (3D) interconnected architectures. The most distinct shape effects are reflected in the density of energy states (DOS). The DOS ($\rho(E)$) of inorganic crystals simultaneously evolves from continuous levels into discrete states as the dimensionality is decreased from 3D to 0D as described by the relationship $\rho(E) \sim E^{(D/2)-1}$ (where D=dimensionality; Fig.3). In 3D crystals, ρ (E) is a smooth square-root function of energy. The 2D crystals confined along a specific direction (e.g. Z axis) show staircase like DOS and 1D crystals confined along two directions (e.g. x, y direction) show saw-tooth like DOS, while 0D crystals show a δ-function like DOS [21].

In recent years, much dedication has been paid to one dimensional (1D) TiO_2 and ZnO nanomaterials such as, nanorods [22] (NRs), nanotubes [16,17] (NTs) and nanofibres [23] (NFs),owing to their superior physical and opto-electronic properties. The surface modification of these 1D TiO_2 nanostructures by adopting appropriate synthetic techniques has opened-up wide range of possibilities for obtaining better photocatalytic activity. The distinct physical properties of 1D nanomaterials, such as, high surface area and mesoporous nature of NTs, [24, 25] superior charge transport property of NFs and large surface area and enhanced surface defects of NRs, [26] make these 1D nanomareials as potential competitors to zero dimensional (0D) nanomaterials (nanoparticles). The quantum confinement of electrons at the nanoscale level assists the rapid and unidirectional transport of photogenerated charge carriers to target pollutants. Furthermore, their high surface-area to volume ratio enables high interfacial charge transfer and mineralization of electron-hole pair recombination with both of these effects being favorable for the photocatalytic degradation reactions [22, 23]. In addition, an introduction of the porous structure in nanotubes to increase the specific surface area represents one way of improving the photocatalytic performance of TiO_2 and ZnO nanostructure materials [27,28]. This structural characteristic provides superior photocatalytic decomposition of organic pollutants because it enables the facile diffusion of organic pollutants into the TiO_2 and ZnO nanostructured materials.

Limitation TiO_2 and ZnO photocatalysts

A good photocatalyst should adsorb the major portion of solar spectrum and should be stable. TiO_2 and ZnO are quite stable photacatalysts against photocorrosion because of theie high energy bandgap (Eg=3.2eV). But they only active in the ultraviolet region which is only <10% of the overall solar spectrum as shown in Fig.4. Also, the photogenerated charge carrier's recombination rate is high in TiO_2 and ZnO. The limitations of the semiconductor photocatalysts can be surmounted by modifying the surface of the semiconductor photocatalysts [54, 61] .

efficient photocatalytic activity, convenient magnetic separation, good stability and recovery[87].

Materials:

Titanium(IV) chloride,Titanium isopropoxide (TTIP), NH_4OH, NaOH, HCl , perchloric acid Ethylene glycol (EG) and polyvinyl pyrrolidene (PVP) were received from Merck chemicals and were used as a starting material for the preparation of TiO_2 nanoparticles (TiO_2 NPs), TiO_2 nanospheres and TiO_2 nanorods. Silver nitrate ($AgNO_3$) (Sigma–Aldrich, 99.9%) was used as a precursor for the preparation of silver nanoparticles and all the other chemicals used in this work were of analytical grade. Unless otherwise mentioned, double distilled water was used for the preparation of aqueous solutions and washings.

III.2. Synthesis of TiO_2 nanoparticles (TiO_2 NPs)

$TiCl_4$ (3 mL) was slowly introduced into double distilled water in an ice bath (0 $^{\circ}$C) under constant stirring until it was completely dissolved and then 6 mL of 30% NH_4OH was added to this suspension .TiO_2 NPs created from(Ti (OH) $_4$). NPs washed with distilled water dried for 3 h

III.3. Synthesis of TiO_2 nanotubes (TiO_2 NTs)

The TiO_2 nanorods (TiO_2 NRs) were prepared as described below: (1) 20 mL of 2N mixed hydroxides (NaOH/KOH = 1:1) was placed in a 50 mL Teflon vessel with a cover for preventing dust, and then, 1 g TiO_2 (commercial TiO_2 nanopowder, Aldrich) was added on the top of the hydroxide in the vessel; (2) the vessel was put into a furnace at 200 °±C for 3 h, the covered vessel was shaken to ensure that the samples were mixed completely and (3) the vessel was kept in the furnace at 200 °C for another 36 h, then washed with 0.1 M HCl solution and distilled water several times till the pH reached 7.0. The final step was the calcination of the obtained sample at different temperatures. In addition, the sample was also prepared following the same procedure but just using water washing for comparison.

III.4. Synthesis of Ag-TiO_2 nanotubes (Ag-TiO_2 NTs)

The silver nanoparticles (Ag NPs) were deposited on the surface of TiO_2 NTs through photo-reduction method [50] in which Ag^+ ions were converted to Ag NPs under UV irradiation.1g of the preformed TiO_2 NTs were dispersed in 250 mL of double distilled water and irradiated with UV light for 10 min to remove the impurities present on their surface. About 4wt% of Ag^+ (i.e., 40 mg of $AgNO_3$) was added into the TiO_2 NTs suspension and the pH was adjusted to 3.5 using perchloric acid,

followed by UV irradiation for 40 min with continuous stirring under N_2 atmosphere. Then, the suspension was filtered, washed thoroughly with double distilled water, dried at 100 ˚C for 3 h and finally calcined at 400 ˚C for 3 h to obtain the Ag-TiO_2 NTs.

III.6. Characterization Studies

Absorprion spectra of different nanostructure of TiO_2-Ag catalyst were recorded using UV-vis spectrophotometer (UV-2550, Shimadzu). Diffuse reflectance spectra (DRS) of different nanocomposites of Ag@TiO_2 and pristine TiO_2 nanoparticles powder were taken using ISR-2200 DRS accessory of UV-vis spectrophotometer (UV-2550, Shimadzu). XRD recorded on Scintag-XDS-2000 diffractometer with Cu .Scanning Electron Microscopy (SEM) images were aquired in TESCAN VEGA3 Scanning Electron Microscope and transmission electron microscopy 200 Kv transition electron microscope. Images were obtained using FEI technique.

III. 7. Photocatalytic activity measurement

Photocatalytic activities of different TiO_2 nanostructures (Ag @TiO_2 NRs and TiO2@Ag NSs) were evaluated by the degradation of methylene blue dye under sunlight irradiation. The reaction cell was placed in a sealed black box with an opening on the top to provide visible-light irradiation. In a typical process, 0.05 g of photocatalyst was added into 100 mL of methylene blue dye with a concentration of 1.05 g L^{-1}. After being dispersed in an ultrasonic bath for 5 min, the solution was stirred for 30 min in the dark to reach the adsorption/desorption equilibrium between the catalyst and the selected methylene blue dye. Then, the suspension was exposed to the sun light irradiation. The samples were collected at given time intervals and the dye concentration was measured by using UV-vis spectroscopy. The experiment was repeated thrice to study the regeneration and reusability of the photocatalyst.

IV Results & Discussion

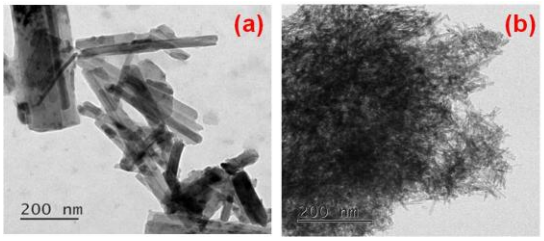

IV.1. Morphology analysis

Fig.1. HRTEM images of prepared TiO_2 nanorods (TiO_2 NRs) (a) and Ag doped TiO_2 nanotubes (Ag@TiO_2NTs) (b).

HRTEM image of a prepared 1D nanostructures of TiO_2 NTs and Ag doped TiO_2 NTs (Ag@TiO_2 NTs) were shown in Figure. a and b. The diameter and length of the NTs were found to be ~50 nm and ~400nm, respectively. The phase and crystal structure of the TiO_2 NTs were confirmed by electron diffraction pattern .The corresponding electron diffraction pattern displays the poly-crystalline nature and could be indexed to the mixed anatase and rutile TiO_2 phase nanostructures. Fig. 1b shows the TEM image of Ag@TiO_2 nanotubes obtained by a hydrothermal method. These nanotube products have an intact tube morphology with an average diameter of ~50nm. As observed from the corresponding diffraction patterns TiO_2 nanotubes possess highly crystallized anatase structure without any impurity phase. which is in good agreement with the obtained XRD pattern .

Furthermore, the diameter of nanowires is about ~20nm. This nanotube structure produces roughly increased surface area which could be beneficial to enhance surface electrochemical reaction. A high resolution transmission electron microscopy (HRTEM) images and the corresponding electron diffraction patterns indicate high crystallinity of the nanotubes

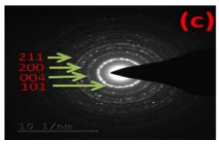

Fig2.. Selected area Electrons diffrection patterns (SEAD) of as-prepared Ag-TiO_2 NTs.

.2. Diffuse Reflectance Spectral Characterization Studies

In the present synthetic chemical reduction method, the formation of the TiO_2 NTs and Ag@TiO_2 NTs nanocomposites take place through the adsorption of Ag+ ions on the TiO_2 chemical reduction of Ag+ of nanostructure is absorved.

The UV-vis diffused reflectance spectra of as-prepared TiO_2 NTs and Ag@TiO_2 NTs composite were recorded. Typically, the TiO_2 did not show any absorbance in the visible region (Fig. 3) because of the wide band gap (~3.2 eV). The deposition of Ag on the TiO_2 surface significantly influenced the absorption in the visible regions of 450 and 550 nm, which was due to the surface plasmon resonance (SPR) band of Ag nanoparticles [33,34]. It can be observed from Fig. 3that the TiO_2 NPs thin film shows its characteristic absorption band arround 390 nm in the UV region of the solar spectrum. The Ag@TiO_2 NTs show highly red shift and covering wavelength around 450 to 550 nm. The intensity of the SPR may be influenced by many factors such as amount of Ag, particle size, dispersion and morphology of Ag nano particles [35], but the peak had a red shift, which means that the metallic Ag particle sizes of TiO_2@Ag are relatively larger than those of TiO_2@Ag NTs [36]. The TiO_2 nanostructures having charecteristic absorption peak of TiO_2, which shows that there is no chemical transformation of the TiO_2 NPs. Moreover, the considerable shift in the adsorption edge toward the visible region was also observed for the Ag@TiO_2 sample. The presence of Ag nanoparticles significantly influenced the visible light absorption properties of TiO_2, which is an essential requirement for obtaining good performance in photocatalytic dye degradation of organic pollutants.

. Diffuse reflectance spectra (DRS) of as prepared TiO_2 NRs (a), TiO_2@Ag NRs (b), TiO_2 NSs (c) TiO_2@Ag NSs (d).

IV.3. X-ray diffraction analysis

The X-ray diffraction (XRD) patterns of the TiO_2 NTs, and TiO_2@Ag NTs were synthesized by the chemical reduction and hydtrothermal methods are shown in Fig. 10. As observed in Fig. 10a and b, all the prepared samples show diffraction peaks at 2θ values of 25.2° (1 0 1), 37.7° (0 0 4), 48.02° (2 0 0), 53.8° (1 0 5), 55.1° (2 1 1), 62.6° (2 0 4), 68.8° (1 1 6), 70.3° (2 2 0) and 75.0° (2 1 5), which were attributed to the anatase TiO_2 (JCPDS, No. 21-1272). In the XRD patterns of Ag@TiO_2 NTs (10a and b), the diffraction peaks at 2θ

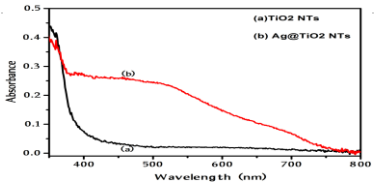

values of 38.7 and 44.7 corresponding to the (111) and (200) crystal faces of the face-centered cubic (fcc) crystalline silver were absent, although the existence of the two crystal faces was confirmed by SAED pattern in TEM (Fig.7). And, we concluded that the absence of XRD peaks of Ag NPs was ascribed to the very small size of Ag NPs , which is in confirms with the reports

.

Fig.4. XRD patterns of as prepaered TiO_2 NTs (a) and Ag@TiO_2 NTs (b).

IV.4. Photocatalytic degradation of methylene blue (MB)

The methylene blue (MB) is one of the most important dyes and has been widely applied in industrial production, which often contaminates the environment. Thus, the photocatalytic performance of the as-synthesized Ag@TiO_2 NTs naocomposites was evaluated by degradation of methylene blue (MB) under direct sun irradiation. The change of absoebance of MB solution at various irradiation times, during the photocatalytic degradation in the presence of the prepared TiO_2 nanostructures, are shown in Fig.1 a&b.

Fig.11a. The absorption spectra of MB recorded at different time intervels during sun light irradiation in the presence of TiO_2 NTs. [Catalyst] = 0.5 g/0.5 L and [MB] = 1.6×10^{-5} M.

The characteristic absorption maximum of MB at 661 nm was

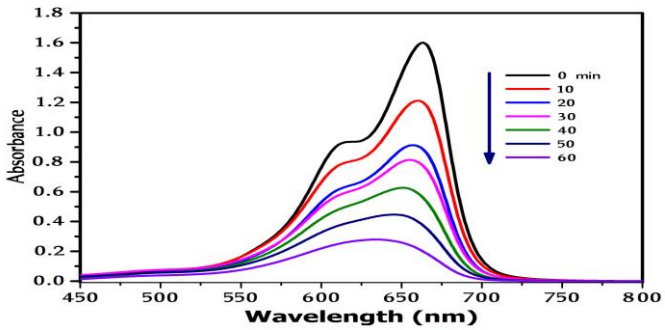

reduced with respect to time, which indicates that MB is photocatalytically decomposed in the presence of as-prepared catalyst Ag-TiO_2 NTs nanocomposites. In the experiments, the degradation efficiency of the as-prepared samples was defined as C/ C_0, where C and C_0 stand for the remnants and initial concentration of MB, respectively. As a reference, the photocatalytic behaviour of Degussa P25 was also measured. Before, the photocatalysis, the solution including MB and prepared catalyst was stirred in the dark for the adsorption equilibrium for 45 min. The photocatalytic performance under sun light for the as-prepared samples including TiO_2 NTs and Ag@TiO_2 NTs, are shown in Fig. 5. The TiO_2-Ag NTs exhibits the highest photocatalytic activity; the average degradation rate of MB is 99.7% within 60 min compared to TiO2 NTs. This may be due to the better crystallinity and good interaction between the Ag and TiO_2 .The order of photocatalytic activity for the samples can be summarized as follows: TiO_2@Ag NTs > TiO_2 NTs. In contrast, the photocatalytic activity of TiO_2 NTs is low; making almost 79% MB remaind in the solution within the same 60 min.

Fig.1b. The absorption spectra of MB recorded at different time intervels during sun light irradiation in the presence of Ag@TiO_2 NTs. [Catalyst] = 0.5 g/0.5 L and [MB] = 1.6×10^{-5}M.

Fig.2. Photocatalytic degradation of methylene blue (MB) in the presence of different catalysts under sunlight irradiation. [Catalyst] = 0.5 g/0.5 L and [MB] = 1.6×10^{-5} M.

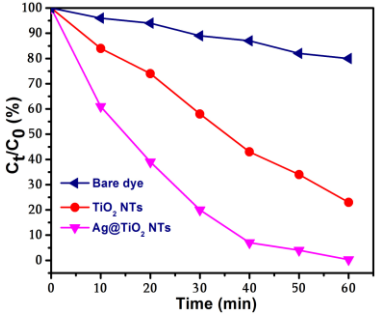

Fig.3. $\ln(C_0/C_t)$ Vs time plots for the photocatalytic degradation of MB over synthesized composites.

The plot of $\ln(C_0/C_t)$ against the light irradiation time (Fig.13) gives a straight line which shows the pseudo first order nature of the reaction and the apparent degradation rate constant was calculated using first-order rate equation ($\ln(C_0/Ct) = k1t$).

Summary & Conclusion

In summary, the TiO_2 NTs and $Ag@TiO_2$ NTs nanocomposites are synthesized via a simple reduction method. Importantly, the synthesized $Ag@TiO_2$ NTs composites exhibit excellent photocatalytic performance under visible light compared to TiO_2 NTs. Furthermore, the improvement of photocatalytic property mainly resulted from the favorable dispersibility of Ag nanoparticles in composites. In this $Ag@TiO_2$ heterojunction nanostructure, Ag could (i) extend the response of composite to visible light and (ii) improve the rapid electron transfer and inhibit the charge recombination. Therefore, the synthesis of high photocatalytic active of Ag-TiO_2 NTs composites will open up a broader range of photocatalytic applications. Hence, it is hopeful to use $Ag@TiO_2$ NTs as an effective photocatalyst in the degradation of organic contaminates to cleanup of aqueous contaminates, especially the aqueous contaminates of dye and so on in the fields of environmental decontamination.

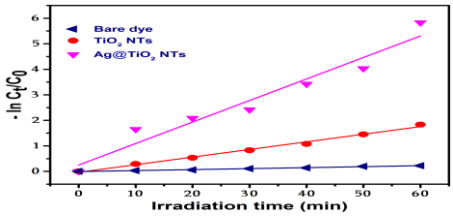

References

1. Hashim, M.A.; Mukhopadhyay, S.; Sahu, J.N.; and Sengupta, B.; Remediation Technologies for Heavy Metal Contaminated Groundwater, *J. Environ. Manage*, **2011**, 92, 2355-2388.
2. Sivakumar, R.; Thomas, J.; and Yoon, M.; Polyoxometalate-based Molecular/Nano Composites: Advances in Environmental Remediation by Photocatalysis and Biomimetic Approaches to Solar Energy Conversion, *J. Photochem. Photobiol. C Photochem. Rev*, **2012**, 13, 277-298.
3. Ahmed, S.; Rasul, M.G.; Brown, R.; and Hashib, M.A.; Influence of Parameters on the Heterogeneous Photocatalytic Degradation of Pesticides and Phenolic Contaminants in wastewater, *J. Environ. Manage*, **2011**, 92, 311-330.
4. Mills, A.; Davies, R.H.; and Worsley, D.; Water Purification by Semiconductor Photocatalysis, *Chem. Soc. Rev*, **1993**, 22, 417-425.
5. Banerjee, S.; Gopal, J.; Muraleedharan, P.; Tyagi, A.K.; and Raj, B.; Physics and Chemistry of Photocatalytic Titanium Dioxide:Visualization of Bactericidal Activity Using Atomic Force Microscopy, *Curr Sci*,**2006**, 90, 1378-1381.
6. Nowotny, J.; Titanium Dioxide-Based Semiconductors for Solar-driven Environmentally Friendly Applications:

Impact of Point Defects on Performance, *Energy Environ. Sci*, **2008**, 1, 565-572.
7. Cazoir, D.; Fine, L.; Ferronato, C.; and Chovelon, J.M.; HydrocarbonRemoval from Bilgewater by a Combination of Air-stripping and Photocatalysis, J. *Hazard. Mater*, **2012**, 235-236, 159-168.
8. Ollis, D.F.; Hsiao, C.Y.; Budiman, L.; and Lee, C.L.; Heterogeneous Photoassisted catalysis: Conversions of Perchloroethylene, Dichloroethane, Chloroacetic acids, and Chlorobenzenes, *J. Catal*, **1984**, 88, 89-96.
9. Matthews, R.W.; Photocatalytic Oxidation of Chlorobenzene in Aqueous Suspensions of Titanium dioxide, *J. Catal*, **1986**, 97, 565-568.
10. Draper, R.B.; and Fox, M.A.; Titanium Dioxide Photosensitized Reactions Studied by Diffuse Reflectance Flash Photolysis in Aqueous Suspensions of TiO_2 Powder, *Langmuir*, **1990,** 6, 1396-1402.
11. Turchi, C.S.; and Ollis, D.F.; Mixed Reactant Photocatalysis: Intermediates and Mutual Rate Inhibition, *J. Catal*, **1989**, 119, 483-496.
12. Turchi, C.S.; and Ollis, D.F.; Photocatalytic Degradation of Organic Water Contaminants: Mechanisms Involving HydroxylRadical Attack, *J Catal*, **1990**, 122, 178-192.
13. Murakami, N.; Katayama, S.; Nakamura, M.; Tsubota, T.; and Ohno, T.; Dependence of Photocatalytic Activity on Aspect Ratio of Shape-Controlled RutileTitanium (IV) Oxide Nanorods, *J. Phys. Chem. C,***2011**, 115, 419-424.
14. Zhu, K.; Neale, N.R.; Miedaner, A.; and Frank, A.J.; Enhanced Charge-Collection Efficiencies and Light Scattering in Dye-Sensitized Solar Cells Using Oriented TiO_2 Nanotubes Arrays, *Nano Lett*, **2007**, 7, 69-74.
15. Bavykin, D.V.; Friedrich, J.M.; and Walsh, F.C.; Protonated Titanates and TiO_2 Nanostructured Materials: Synthesis, Properties, and Applications, *Adv. Mater*, **2006**, 18, 2807-2824.
16. Zhou, H.; Qu, Y.; Zeid, T.; and Duan, X.; Towards Highly Efficient Photocatalysts Using Semiconductor Nanoarchitectures,*Energy Environ. Sci*, **2012**, 5, 6732-6743.
17. Yun, H.J.; Lee, H.; Joo, J.B.; Kim, W.; and Yi, J.; Influence of Aspect Ratio of TiO_2 Nanorods on the Photocatalytic Decomposition of FormicAcid, *J. Phys. Chem. C*, **2009**, 113, 3050-3055.
18. Wu, J.M.; Zhang, T.W.; Zeng, Y.W.; Hayakawa, S.; Tsuru, K.; and Osaka, A.;Large-Scale Preparation of Ordered Titania Nanorods withEnhanced Photocatalytic Activity, *Langmuir*, **2005**, 21, 6995-7002.
19. Zhao, T.; Liu, Z.; Nakata, K.; Nishimoto, S.; Murakami, T.; Zhao, Y.; Jiang, L.; and Fujishima, A.; Multichannel TiO2 Hollow Fibers with Enhanced Photocatalytic Activity, *J. Mater. Chem*, **2010**, 20, 5095-5099.
20. Zhong, L.S.; Hu, J.S.; Wan, L.J.; and Song, W.G.; Facile Synthesis of Nanoporous Anatase Spheres and Their Environmental Applications, *Chem. Commun*, **2008,** 1184-1186.
21. Wang, X.; and Caruso, R.A.; Enhancing Photocatalytic Activity of Titania

Materials by Using Porous Structures and the Addition of Gold Nanoparticles, *J. Mater. Chem*, **2011**, 21, 20-28.

22. Anandan, S.; Kumar, P.S.; Pugazhenthiran, N.; Madhavan, J.; and Maruthamuthu, P.; Effect of Loaded Silver Nanoparticles on TiO_2 for Photocatalytic Degradation of Acid Red 88, *Sol. Energy Mater. Sol. Cells*, **2008**, 92,929-937.
23. Tian, Y.; and Tatsuma, T.; Plasmon-Induced Photoelectrochemistry at Metal Nanoparticles Supported on Nanoporous TiO_2, *Chem. Commun*, **2004**,1810-1811.
24. Tian, Y.; and Tatsuma, T.; Mechanisms and Applications of Plasmon-Induced Charge Separation at TiO_2 Films Loaded with Gold Nanoparticles,*J. Am. Chem. Soc*, **2005**, 127, 7632-7637.
25. Kuhnlein, H.V.; and Chan, H.M.; Environment and Contaminants In Traditional Food Systems Of Northern Indigenous Peoples, *Annu. Rev. Nutr*, **2000**, 20**,** 595-626.
26. Kummerer, K.; Drugs in the Environment: Emission of Drugs, Diagnostic Aids and Disinfectants into Wastewater by Hospitals in Relation to Other Sources, *Chemosphere*, **2001**, 45, 957-969.
27. Kominami, H.; Tanaka, A.; and Hashimoto, K.;Mineralization of Organic Acids in Aqueous Suspensions of Gold Nanoparticles Supported on Cerium(IV) Oxide Powder Under Visible Light Irradiation, *Chem. Commun*,**2010**,46,1287-1289.
28. Photiphitak, C.; Rakkwamsuk, P.; Muthitamongkol, P.; SaeKung, C.; and Thanachayanont, C.; *Int. J. Photoenergy*, 2011, 357-979.
29. Tian, Z.; Wang, L.; Jia, L.; Li, Q.; Song, Q.; Su, S.; and Yang, H.;A Novel Biomass Coated Ag–TiO_2 Composite as a Photoanode for Enhanced Photocurrent in dye-sensitized solar cells, *RSC Adv*,**2013**, 3, 6369– 6376.
30. Link, S.; and El-Sayed,M. A.; Spectral Properties and Relaxation Dynamics of Surface Plasmon Electronic Oscillations in Gold and Silver Nanodots and Nanorods*J. Phys. Chem. B*, **1999**,103, 8410–8426.
31. Tseng, I. H.; and Wu,J. C. S.;Chemical states of metal-loaded titania in the photoreduction of CO_2, *Catal. Today*, **2004,** 97, 113–119.